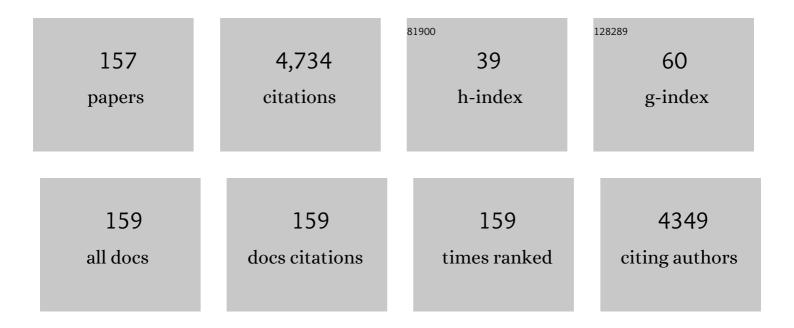
Oliver Langer

List of Publications by Year in descending order

Source: https://exaly.com/author-pdf/4334247/publications.pdf Version: 2024-02-01



#	Article	lF	CITATIONS
1	Comparative vulnerability of PET radioligands to partial inhibition of P-glycoprotein at the blood-brain barrier: A criterion of choice?. Journal of Cerebral Blood Flow and Metabolism, 2022, 42, 175-185.	4.3	14
2	PET imaging to assess the impact of P-glycoprotein on pulmonary drug delivery in rats. Journal of Controlled Release, 2022, 342, 44-52.	9.9	11
3	Microdosing as a Potential Tool to Enhance Clinical Development of Novel Antibiotics: A Tissue and Plasma PK Feasibility Study with Ciprofloxacin. Clinical Pharmacokinetics, 2022, , 1.	3.5	5
4	Pharmacokinetic Imaging Using 99mTc-Mebrofenin to Untangle the Pattern of Hepatocyte Transporter Disruptions Induced by Endotoxemia in Rats. Pharmaceuticals, 2022, 15, 392.	3.8	2
5	Strategic, feasibility, economic, and cultural aspects of phase 0 approaches. Clinical and Translational Science, 2022, 15, 1355-1379.	3.1	6
6	Use of PET Imaging to Assess the Efficacy of Thiethylperazine to Stimulate Cerebral MRP1 Transport Activity in Wild-Type and APP/PS1-21 Mice. International Journal of Molecular Sciences, 2022, 23, 6514.	4.1	2
7	Impact of P-gp and BCRP on pulmonary drug disposition assessed by PET imaging in rats. Journal of Controlled Release, 2022, 349, 109-117.	9.9	5
8	Complete inhibition of ABCB1 and ABCG2 at the blood–brain barrier by co-infusion of erlotinib and tariquidar to improve brain delivery of the model ABCB1/ABCG2 substrate [¹¹ C]erlotinib. Journal of Cerebral Blood Flow and Metabolism, 2021, 41, 1634-1646.	4.3	17
9	Influence of Cation Transporters (OCTs and MATEs) on the Renal and Hepatobiliary Disposition of [11C]Metoclopramide in Mice. Pharmaceutical Research, 2021, 38, 127-140.	3.5	1
10	Repurposing 99mTc-Mebrofenin as a Probe for Molecular Imaging of Hepatocyte Transporters. Journal of Nuclear Medicine, 2021, 62, 1043-1047.	5.0	4
11	Imaging-Based Characterization of a Slco2b1(-/-) Mouse Model Using [11C]Erlotinib and [99mTc]Mebrofenin as Probe Substrates. Pharmaceutics, 2021, 13, 918.	4.5	2
12	ABCB1 and ABCG2 Together Limit the Distribution of ABCB1/ABCG2 Substrates to the Human Retina and the ABCG2 Single Nucleotide Polymorphism Q141K (c.421C> A) May Lead to Increased Drug Exposure. Frontiers in Pharmacology, 2021, 12, 698966.	3.5	6
13	Assessing the Functional Redundancy between P-gp and BCRP in Controlling the Brain Distribution and Biliary Excretion of Dual Substrates with PET Imaging in Mice. Pharmaceutics, 2021, 13, 1286.	4.5	7
14	Influence of ABC transporters on the excretion of ciprofloxacin assessed with PET imaging in mice. European Journal of Pharmaceutical Sciences, 2021, 163, 105854.	4.0	7
15	Human Biodistribution and Radiation Dosimetry of the P-Glycoprotein Radiotracer [11C]Metoclopramide. Molecular Imaging and Biology, 2021, 23, 180-185.	2.6	0
16	Impaired Clearance From the Brain Increases the Brain Exposure to Metoclopramide in Elderly Subjects. Clinical Pharmacology and Therapeutics, 2021, 109, 754-761.	4.7	13
17	Age dependency of cerebral P-glycoprotein function in wild-type and APPPS1 mice measured with PET. Journal of Cerebral Blood Flow and Metabolism, 2020, 40, 150-162.	4.3	20
18	Measurement of cerebral ABCC1 transport activity in wild-type and APP/PS1-21 mice with positron emission tomography. Journal of Cerebral Blood Flow and Metabolism, 2020, 40, 954-965.	4.3	14

#	Article	IF	CITATIONS
19	In vivo characterization of [18F]AVT-011 as a radiotracer for PET imaging of multidrug resistance. European Journal of Nuclear Medicine and Molecular Imaging, 2020, 47, 2026-2035.	6.4	3
20	Pharmacokinetic Imaging with Radiolabeled Molecularly Targeted Anticancer Drugs. Journal of Nuclear Medicine, 2020, 61, 306-306.	5.0	0
21	Imaging P-Glycoprotein Induction at the Blood–Brain Barrier of a β-Amyloidosis Mouse Model with ¹¹ C-Metoclopramide PET. Journal of Nuclear Medicine, 2020, 61, 1050-1057.	5.0	21
22	Measurement of Hepatic ABCB1 and ABCG2 Transport Activity with [11C]Tariquidar and PET in Humans and Mice. Molecular Pharmaceutics, 2020, 17, 316-326.	4.6	15
23	Brain Distribution of Dual ABCB1/ABCG2 Substrates Is Unaltered in a Beta-Amyloidosis Mouse Model. International Journal of Molecular Sciences, 2020, 21, 8245.	4.1	4
24	Tobacco Smoke and Inhaled Drugs Alter Expression and Activity of Multidrug Resistance-Associated Protein-1 (MRP1) in Human Distal Lung Epithelial Cells in vitro. Frontiers in Bioengineering and Biotechnology, 2020, 8, 1030.	4.1	12
25	Phase 0/microdosing approaches: time for mainstream application in drug development?. Nature Reviews Drug Discovery, 2020, 19, 801-818.	46.4	55
26	Validation of Pharmacological Protocols for Targeted Inhibition of Canalicular MRP2 Activity in Hepatocytes Using [99mTc]mebrofenin Imaging in Rats. Pharmaceutics, 2020, 12, 486.	4.5	7
27	Use of imaging to assess the activity of hepatic transporters. Expert Opinion on Drug Metabolism and Toxicology, 2020, 16, 149-164.	3.3	17
28	Assessing the Activity of Multidrug Resistance–Associated Protein 1 at the Lung Epithelial Barrier. Journal of Nuclear Medicine, 2020, 61, 1650-1657.	5.0	16
29	Proof-of-Concept Study of Drug Brain Permeability Between in Vivo Human Brain and an in Vitro iPSCs-Human Blood-Brain Barrier Model. Scientific Reports, 2019, 9, 16310.	3.3	42
30	Inhibition of ABCB1 and ABCG2 at the Mouse Blood–Brain Barrier with Marketed Drugs To Improve Brain Delivery of the Model ABCB1/ABCG2 Substrate [¹¹ C]erlotinib. Molecular Pharmaceutics, 2019, 16, 1282-1293.	4.6	20
31	Generation and Characterization of an <i>Abcc1</i> Humanized Mouse Model (<i>hABCC1^{flx/flx}</i>) with Knockout Capability. Molecular Pharmacology, 2019, 96, 138-147.	2.3	4
32	Towards Improved Pharmacokinetic Models for the Analysis of Transporter-Mediated Hepatic Disposition of Drug Molecules with Positron Emission Tomography. AAPS Journal, 2019, 21, 61.	4.4	14
33	Imaging Pâ€Glycoprotein Function at the Blood–Brain Barrier as a Determinant of the Variability in Response to Central Nervous System Drugs. Clinical Pharmacology and Therapeutics, 2019, 105, 1061-1064.	4.7	25
34	PET imaging of the mouse brain reveals a dynamic regulation of SERT density in a chronic stress model. Translational Psychiatry, 2019, 9, 80.	4.8	7
35	Impact of P-Glycoprotein Function on the Brain Kinetics of the Weak Substrate ¹¹ C-Metoclopramide Assessed with PET Imaging in Humans. Journal of Nuclear Medicine, 2019, 60, 985-991.	5.0	38
36	Influence of Multidrug Resistance-Associated Proteins on the Excretion of the ABCC1 Imaging Probe 6-Bromo-7-[11C]Methylpurine in Mice. Molecular Imaging and Biology, 2019, 21, 306-316.	2.6	15

#	Article	IF	CITATIONS
37	A Proof-of-Concept Study to Inhibit ABCC2- and ABCB1-Mediated Efflux Transport at the Human Blood–Brain Barrier. Journal of Nuclear Medicine, 2019, 60, 486-491.	5.0	25
38	Assessment of brain delivery of a model ABCB1/ABCG2 substrate in patients with non-contrast-enhancing brain tumors with positron emission tomography. EJNMMI Research, 2019, 9, 110.	2.5	2
39	Pitfalls and solutions of the fully-automated radiosynthesis of [11C]metoclopramide. EJNMMI Radiopharmacy and Chemistry, 2019, 4, 31.	3.9	7
40	Investigation of Transporter-Mediated Drug-Drug Interactions Using PET/MRI. , 2019, , 117-133.		0
41	Imaging techniques to study drug transporter function in vivo. , 2018, 189, 104-122.		57
42	Pharmacokinetics of the P-gp Inhibitor Tariquidar in Rats After Intravenous, Oral, and Intraperitoneal Administration. European Journal of Drug Metabolism and Pharmacokinetics, 2018, 43, 599-606.	1.6	18
43	Influence of breast cancer resistance protein and P-glycoprotein on tissue distribution and excretion of Ko143 assessed with PET imaging in mice. European Journal of Pharmaceutical Sciences, 2018, 115, 212-222.	4.0	4
44	Intravenous infusion for the controlled exposure to the dual ABCB1 and ABCG2 inhibitor elacridar in nonhuman primates. Drug Delivery and Translational Research, 2018, 8, 536-542.	5.8	7
45	Influence of OATPs on Hepatic Disposition of Erlotinib Measured With Positron Emission Tomography. Clinical Pharmacology and Therapeutics, 2018, 104, 139-147.	4.7	43
46	PET-MR and SPECT-MR multimodality probes: Development and challenges. Theranostics, 2018, 8, 6210-6232.	10.0	59
47	Comparison of fully-automated radiosyntheses of [11C]erlotinib for preclinical and clinical use starting from in target produced [11C]CO2 or [11C]CH4. EJNMMI Radiopharmacy and Chemistry, 2018, 3, 8.	3.9	10
48	EGFR is required for FOSâ€dependent bone tumor development via RSK2/CREB signaling. EMBO Molecular Medicine, 2018, 10, .	6.9	24
49	Humanization of the blood–brain barrier transporter ABCB1 in mice disrupts genomic locus — lessons from three unsuccessful approaches. European Journal of Microbiology and Immunology, 2018, 8, 78-86.	2.8	2
50	Liver Imaging and Hepatobiliary Contrast Media. Contrast Media and Molecular Imaging, 2018, 2018, 1-2.	0.8	1
51	Molar activity – The keystone in 11C-radiochemistry: An explorative study using the gas phase method. Nuclear Medicine and Biology, 2018, 67, 21-26.	0.6	4
52	Effect of Rifampicin on the Distribution of [¹¹ C]Erlotinib to the Liver, a Translational PET Study in Humans and in Mice. Molecular Pharmaceutics, 2018, 15, 4589-4598.	4.6	17
53	Impact of rifampicin-inhibitable transport on the liver distribution and tissue kinetics of erlotinib assessed with PET imaging in rats. EJNMMI Research, 2018, 8, 81.	2.5	8
54	P-Glycoprotein (ABCB1) Inhibits the Influx and Increases the Efflux of ¹¹ C-Metoclopramide Across the Blood–Brain Barrier: A PET Study on Nonhuman Primates. Journal of Nuclear Medicine, 2018, 59, 1609-1615.	5.0	39

#	Article	IF	CITATIONS
55	Effect of Pâ€glycoprotein inhibition at the blood–brain barrier on brain distribution of (<i>R</i>)â€{ ¹¹ C]verapamil in elderly <i>vs.</i> young subjects. British Journal of Clinical Pharmacology, 2017, 83, 1991-1999.	2.4	28
56	A Prediction Method for P-glycoprotein–Mediated Drug–Drug Interactions at the Human Blood–Brain Barrier From Blood Concentration–Time Profiles, Validated With PET Data. Journal of Pharmaceutical Sciences, 2017, 106, 2780-2786.	3.3	4
57	PET probes for imaging pancreatic islet cells. Clinical and Translational Imaging, 2017, 5, 507-523.	2.1	5
58	Hepatocyte-Specific Deletion of EGFR in Mice Reduces Hepatic Abcg2 Transport Activity Measured by [11C]erlotinib and Positron Emission Tomography. Drug Metabolism and Disposition, 2017, 45, 1093-1100.	3.3	11
59	Expression of endogenous mouse APP modulates β-amyloid deposition in hAPP-transgenic mice. Acta Neuropathologica Communications, 2017, 5, 49.	5.2	21
60	Assessment of P-Glycoprotein Transport Activity at the Human Blood–Retina Barrier with (<i>R</i>)â€ ¹¹ C-Verapamil PET. Journal of Nuclear Medicine, 2017, 58, 678-681.	5.0	23
61	On the applicability of [18F]FBPA to predict L-BPA concentration after amino acid preloading in HuH-7 liver tumor model and the implication for liver boron neutron capture therapy. Nuclear Medicine and Biology, 2017, 44, 83-89.	0.6	14
62	Strategies to Inhibit ABCB1- and ABCG2-Mediated Efflux Transport of Erlotinib at the Blood–Brain Barrier: A PET Study on Nonhuman Primates. Journal of Nuclear Medicine, 2017, 58, 117-122.	5.0	43
63	Reproducibility of Quantitative Brain Imaging Using a PET-Only and a Combined PET/MR System. Frontiers in Neuroscience, 2017, 11, 396.	2.8	8
64	[11 C]Erlotinib PET cannot detect acquired erlotinib resistance in NSCLC tumor xenografts in mice. Nuclear Medicine and Biology, 2017, 52, 7-15.	0.6	6
65	32nd International Austrian Winter Symposium. EJNMMI Research, 2016, 6, 32.	2.5	Ο
66	Synthesis and preclinical characterization of 1-(6′-deoxy-6′-[18 F]fluoro-β- d) Tj ETQq0 0 0 rgBT /Overlock assess tumor hypoxia. Bioorganic and Medicinal Chemistry, 2016, 24, 5326-5339.	10 Tf 50 3 3.0	307 Td (-allofu 13
67	Preloading with L-BPA, L-tyrosine and L-DOPA enhances the uptake of [18F]FBPA in human and mouse tumour cell lines. Applied Radiation and Isotopes, 2016, 118, 67-72.	1.5	12
68	Use of PET Imaging to Evaluate Transporterâ€Mediated Drugâ€Drug Interactions. Journal of Clinical Pharmacology, 2016, 56, S143-56.	2.0	48
69	Pilot PET Study to Assess the Functional Interplay Between ABCB1 and ABCG2 at the Human Blood–Brain Barrier. Clinical Pharmacology and Therapeutics, 2016, 100, 131-141.	4.7	50
70	Whole-Body Distribution and Radiation Dosimetry of ¹¹ C-Elacridar and ¹¹ C-Tariquidar in Humans. Journal of Nuclear Medicine, 2016, 57, 1265-1268.	5.0	11
71	Influence of 24-Nor-Ursodeoxycholic Acid on Hepatic Disposition of [18F]Ciprofloxacin, a Positron Emission Tomography Study in Mice. Journal of Pharmaceutical Sciences, 2016, 105, 106-112.	3.3	5
72	Generation and Characterization of a Breast Cancer Resistance Protein Humanized Mouse Model. Molecular Pharmacology, 2016, 89, 492-504.	2.3	23

#	Article	IF	CITATIONS
73	Tools in Clinical Pharmacology: Imaging Techniques. , 2016, , 139-150.		1
74	[18F]FE@SUPPY: a suitable PET tracer for the adenosine A3 receptor? An in vivo study in rodents. European Journal of Nuclear Medicine and Molecular Imaging, 2015, 42, 741-749.	6.4	5
75	Factors Governing P-Glycoprotein-Mediated Drug–Drug Interactions at the Blood–Brain Barrier Measured with Positron Emission Tomography. Molecular Pharmaceutics, 2015, 12, 3214-3225.	4.6	39
76	[18F]FDG is not transported by P-glycoprotein and breast cancer resistance protein at the rodent blood–brain barrier. Nuclear Medicine and Biology, 2015, 42, 585-589.	0.6	2
77	Development of Fluorine-18 Labeled Metabolically Activated Tracers for Imaging of Drug Efflux Transporters with Positron Emission Tomography. Journal of Medicinal Chemistry, 2015, 58, 6058-6080.	6.4	18
78	Automated electrophilic radiosynthesis of [18F]FBPA using a modified nucleophilic GE TRACERlab FXFDG. Applied Radiation and Isotopes, 2015, 104, 124-127.	1.5	9
79	Approaching Complete Inhibition of P-Glycoprotein at the Human Blood–Brain Barrier: An (<i>R</i>)-[¹¹ C]Verapamil PET Study. Journal of Cerebral Blood Flow and Metabolism, 2015, 35, 743-746.	4.3	74
80	Development and performance test of an online blood sampling system for determination of the arterial input function in rats. EJNMMI Physics, 2015, 2, 1.	2.7	22
81	Automated radiosynthesis of [18F]ciprofloxacin. Applied Radiation and Isotopes, 2015, 99, 133-137.	1.5	5
82	Breast Cancer Resistance Protein and P-Glycoprotein Influence In Vivo Disposition of ¹¹ C-Erlotinib. Journal of Nuclear Medicine, 2015, 56, 1930-1936.	5.0	52
83	Role of (Drug) Transporters in Imaging in Health and Disease. Drug Metabolism and Disposition, 2014, 42, 2007-2015.	3.3	11
84	Alzheimer's and ABC transporters — new opportunities for diagnostics and treatment. Neurobiology of Disease, 2014, 72, 54-60.	4.4	66
85	In vivo P-glycoprotein function before and after epilepsy surgery. Neurology, 2014, 83, 1326-1331.	1.1	37
86	Using Positron Emission Tomography to Study Transporter-Mediated Drug–Drug Interactions in Tissues. Clinical Pharmacology and Therapeutics, 2014, 96, 206-213.	4.7	31
87	(R)-[11C]verapamil is selectively transported by murine and human P-glycoprotein at the blood–brain barrier, and not by MRP1 and BCRP. Nuclear Medicine and Biology, 2013, 40, 873-878.	0.6	67
88	Tariquidar and Elacridar Are Dose-Dependently Transported by P-Glycoprotein and Bcrp at the Blood-Brain Barrier: A Small-Animal Positron Emission Tomography and In Vitro Study. Drug Metabolism and Disposition, 2013, 41, 754-762.	3.3	79
89	Complementary Techniques: Positron Emission Tomography. AAPS Advances in the Pharmaceutical Sciences Series, 2013, , 269-282.	0.6	0
90	Assessment of cerebral P-glycoprotein expression and function with PET by combined [11C]inhibitor and [11C]substrate scans in rats. Nuclear Medicine and Biology, 2013, 40, 755-763.	0.6	15

#	Article	IF	CITATIONS
91	P-glycoprotein expression and function in patients with temporal lobe epilepsy: a case-control study. Lancet Neurology, The, 2013, 12, 777-785.	10.2	155
92	Factors That Limit Positron Emission Tomography Imaging of P-Glycoprotein Density at the Blood–Brain Barrier. Molecular Pharmaceutics, 2013, 10, 2222-2229.	4.6	18
93	Interaction of ¹¹ C-Tariquidar and ¹¹ C-Elacridar with P-Glycoprotein and Breast Cancer Resistance Protein at the Human Blood–Brain Barrier. Journal of Nuclear Medicine, 2013, 54, 1181-1187.	5.0	45
94	Radioligands targeting Pâ€glycoprotein and other drug efflux proteins at the blood–brain barrier. Journal of Labelled Compounds and Radiopharmaceuticals, 2013, 56, 68-77.	1.0	45
95	A Novel PET Protocol for Visualization of Breast Cancer Resistance Protein Function at the Blood–Brain Barrier. Journal of Cerebral Blood Flow and Metabolism, 2012, 32, 2002-2011.	4.3	46
96	Blood–brain barrier P-glycoprotein function in Alzheimer's disease. Brain, 2012, 135, 181-189.	7.6	252
97	Interaction of HM30181 with P-glycoprotein at the murine blood–brain barrier assessed with positron emission tomography. European Journal of Pharmacology, 2012, 696, 18-27.	3.5	9
98	Synthesis and preclinical evaluation of the radiolabeled P-glycoprotein inhibitor [11C]MC113. Nuclear Medicine and Biology, 2012, 39, 1219-1225.	0.6	17
99	Pgp-Mediated Interaction Between (R)-[11C]Verapamil and Tariquidar at the Human Blood–Brain Barrier: A Comparison With Rat Data. Clinical Pharmacology and Therapeutics, 2012, 91, 227-233.	4.7	108
100	Pharmacokinetic modeling of P-glycoprotein function at the rat and human blood–brain barriers studied with (R)-[11C]verapamil positron emission tomography. EJNMMI Research, 2012, 2, 58.	2.5	16
101	The antiepileptic drug mephobarbital is not transported by P-glycoprotein or multidrug resistance protein 1 at the blood–brain barrier: A positron emission tomography study. Epilepsy Research, 2012, 100, 93-103.	1.6	12
102	A comparative small-animal PET evaluation of [11C]tariquidar, [11C]elacridar and (R)-[11C]verapamil for detection of P-glycoprotein-expressing murine breast cancer. European Journal of Nuclear Medicine and Molecular Imaging, 2012, 39, 149-159.	6.4	23
103	A Combined Accelerator Mass Spectrometry-Positron Emission Tomography Human Microdose Study with 14C- and 11C-Labelled Verapamil. Clinical Pharmacokinetics, 2011, 50, 111-120.	3.5	31
104	PET and SPECT Radiotracers to Assess Function and Expression of ABC Transporters In Vivo. Current Drug Metabolism, 2011, 12, 774-792.	1.2	59
105	Approaches using molecular imaging technology — use of PET in clinical microdose studies. Advanced Drug Delivery Reviews, 2011, 63, 539-546.	13.7	102
106	Radiosynthesis and Assessment of Ocular Pharmacokinetics of 124I-Labeled Chitosan in Rabbits Using Small-Animal PET. Molecular Imaging and Biology, 2011, 13, 222-226.	2.6	19
107	Radiosynthesis and in vivo evaluation of 1-[18F]fluoroelacridar as a positron emission tomography tracer for P-glycoprotein and breast cancer resistance protein. Bioorganic and Medicinal Chemistry, 2011, 19, 2190-2198.	3.0	30
108	Gastric Cancer Growth Control by BEZ235 <i>In Vivo</i> Does Not Correlate with PI3K/mTOR Target Inhibition but with [18F]FLT Uptake. Clinical Cancer Research, 2011, 17, 5322-5332.	7.0	33

#	Article	IF	CITATIONS
109	A Novel Positron Emission Tomography Imaging Protocol Identifies Seizure-Induced Regional Overactivity of P-Glycoprotein at the Blood-Brain Barrier. Journal of Neuroscience, 2011, 31, 8803-8811.	3.6	58
110	Dose-response assessment of tariquidar and elacridar and regional quantification of P-glycoprotein inhibition at the rat blood-brain barrier using (R)-[11C]verapamil PET. European Journal of Nuclear Medicine and Molecular Imaging, 2010, 37, 942-953.	6.4	102
111	Synthesis and in vivo evaluation of [11C]tariquidar, a positron emission tomography radiotracer based on a third-generation P-glycoprotein inhibitor. Bioorganic and Medicinal Chemistry, 2010, 18, 5489-5497.	3.0	73
112	Small-animal PET evaluation of [11C]MC113 as a PET tracer for P-glycoprotein. BMC Pharmacology, 2010, 10, .	0.4	0
113	Dose-response assessment of tariquidar for inhibition of P-glycoprotein at the human blood-brain barrier using (R)-[11C]verapamil PET. BMC Pharmacology, 2010, 10, .	0.4	0
114	Assessment of Regional Differences in Tariquidar-Induced P-Glycoprotein Modulation at the Human Blood–Brain Barrier. Journal of Cerebral Blood Flow and Metabolism, 2010, 30, 510-515.	4.3	34
115	Imaging of P-glycoprotein Function and Expression to Elucidate Mechanisms of Pharmacoresistance in Epilepsy. Current Topics in Medicinal Chemistry, 2010, 10, 1785-1791.	2.1	40
116	Evaluation of [11C]elacridar and [11C]tariquidar in transporter knockout mice using small-animal PET. NeuroImage, 2010, 52, S25.	4.2	3
117	Synthesis and in vivo evaluation of the putative breast cancer resistance protein inhibitor [11C]methyl 4-((4-(2-(6,7-dimethoxy-1,2,3,4-tetrahydroisoquinolin-2-yl)ethyl)phenyl)amino-carbonyl)-2-(quinoline-2-carbonyl Nuclear Medicine and Biology, 2010, 37, 637-644.	ami o œ)ben	zoatæ.
118	Tools in clinical pharmacology - imaging techniques. , 2010, , 193-203.		0
119	A Pilot Study to Assess the Efficacy of Tariquidar to Inhibit P-glycoprotein at the Human Blood–Brain Barrier with (<i>R</i>)- ¹¹ C-Verapamil and PET. Journal of Nuclear Medicine, 2009, 50, 1954-1961.	5.0	99
120	Limitations of Small Animal PET Imaging with [18F]FDDNP and FDG for Quantitative Studies in a Transgenic Mouse Model of Alzheimer's Disease. Molecular Imaging and Biology, 2009, 11, 236-240.	2.6	87
121	Age dependency of cerebral P-gp function measured with (R)-[11C]verapamil and PET. European Journal of Clinical Pharmacology, 2009, 65, 941-946.	1.9	65
122	Synthesis and Small-Animal Positron Emission Tomography Evaluation of [11C]-Elacridar As a Radiotracer to Assess the Distribution of P-Glycoprotein at the Bloodâ^'Brain Barrier. Journal of Medicinal Chemistry, 2009, 52, 6073-6082.	6.4	71
123	New ultrasensitive detection technologies and techniques for use in microdosing studies. Bioanalysis, 2009, 1, 357-366.	1.5	27
124	Peripheral metabolism of (R)-[11C]verapamil in epilepsy patients. European Journal of Nuclear Medicine and Molecular Imaging, 2008, 35, 116-123.	6.4	39
125	Microdosing Studies in Humans. Drugs in R and D, 2008, 9, 73-81.	2.2	42
126	Tariquidar-Induced P-Glycoprotein Inhibition at the Rat Blood–Brain Barrier Studied with (<i>R</i>)- ¹¹ C-Verapamil and PET. Journal of Nuclear Medicine, 2008, 49, 1328-1335.	5.0	104

#	Article	IF	CITATIONS
127	Positron emission tomography for use in microdosing studies. Current Opinion in Drug Discovery & Development, 2008, 11, 104-10.	1.9	12
128	Pharmacoresistance in Epilepsy: A Pilot PET Study with the P-Glycoprotein Substrate R -[11 C]verapamil. Epilepsia, 2007, 48, 1774-1784.	5.1	119
129	A positron emission tomography microdosing study with a potential antiamyloid drug in healthy volunteers and patients with Alzheimer's disease. Clinical Pharmacology and Therapeutics, 2006, 80, 216-227.	4.7	53
130	Microdialysis versus other techniques for the clinical assessment of in vivo tissue drug distribution. AAPS Journal, 2006, 8, E263-E271.	4.4	70
131	Synthesis of fluorine-18-labelled 5- and 6-fluoro-2-pyridinamine. Journal of Labelled Compounds and Radiopharmaceuticals, 2006, 49, 345-356.	1.0	13
132	Microdialysis Versus Other Techniques for the Clinical Assessment of In Vivo Tissue Drug Distribution. AAPS Journal, 2006, 08, E263.	4.4	5
133	Influence of functional haplotypes in the drug transporter gene on central nervous system drug distribution in humans. Clinical Pharmacology and Therapeutics, 2005, 78, 182-190.	4.7	64
134	Synthesis of 1,1′ [11C]-methylene-di-(2-naphthol) ([11C]ST1859) for PET studies in humans. Journal of Labelled Compounds and Radiopharmaceuticals, 2005, 48, 577-587.	1.0	12
135	In vitro and in vivo evaluation of [18F]ciprofloxacin for the imaging of bacterial infections with PET. European Journal of Nuclear Medicine and Molecular Imaging, 2005, 32, 143-150.	6.4	77
136	Combined PET and microdialysis for in vivo assessment of intracellular drug pharmacokinetics in humans. Journal of Nuclear Medicine, 2005, 46, 1835-41.	5.0	35
137	[18 F]Ciprofloxacin, a New Positron Emission Tomography Tracer for Noninvasive Assessment of the Tissue Distribution and Pharmacokinetics of Ciprofloxacin in Humans. Antimicrobial Agents and Chemotherapy, 2004, 48, 3850-3857.	3.2	54
138	Biological evaluation of 2′-[18F]fluoroflumazenil ([18F]FFMZ), a potential GABA receptor ligand for PET. Nuclear Medicine and Biology, 2004, 31, 291-295.	0.6	43
139	Positron emission tomographic evaluation of the putative dopamine-D3 receptor ligand, 611C9RGH-1756 in the monkey brain. Neurochemistry International, 2004, 45, 609-617.	3.8	31
140	A novel electrophilic synthesis and evaluation of medium specific radioactivity (1R,2S)-4-[18F]fluorometaraminol, a tracer for the assessment of cardiac sympathetic nerve integrity with PET. Nuclear Medicine and Biology, 2004, 31, 103-110.	0.6	21
141	Methods to Assess Tissue-Specific Distribution and Metabolism of Drugs. Current Drug Metabolism, 2004, 5, 463-481.	1.2	70
142	Preparation of 4-[11C]methylmetaraminol, a potential PET tracer for assessment of myocardial sympathetic innervation. Journal of Labelled Compounds and Radiopharmaceuticals, 2003, 46, 55-65.	1.0	18
143	A general method for the fluorine-18 labelling of fluoroquinolone antibiotics. Journal of Labelled Compounds and Radiopharmaceuticals, 2003, 46, 715-727.	1.0	10
144	Comparison of three different purification methods for the routine preparation of [11C] Metomidate. Applied Radiation and Isotopes, 2003, 59, 125-128.	1.5	8

#	Article	IF	CITATIONS
145	Synthesis of fluorine-18-labeled ciprofloxacin for PET studies in humans. Nuclear Medicine and Biology, 2003, 30, 285-291.	0.6	123
146	PET and SPET tracers for mapping the cardiac nervous system. European Journal of Nuclear Medicine and Molecular Imaging, 2002, 29, 416-434.	6.4	66
147	Synthesis of high-specific-radioactivity 4- and 6-[18F]fluorometaraminol- PET tracers for the adrenergic nervous system of the heart. Bioorganic and Medicinal Chemistry, 2001, 9, 677-694.	3.0	40
148	Improved specific radioactivity of the PET radioligand [11C]FLB 457 by use of the GE medical systems PETtrace MeI microlab. Journal of Labelled Compounds and Radiopharmaceuticals, 2000, 43, 331-338.	1.0	49
149	Radiochemical labelling of the dopamine D3 receptor ligand RGH-1756. Journal of Labelled Compounds and Radiopharmaceuticals, 2000, 43, 1069-1074.	1.0	10
150	Preparation of [18F]β-CFT-FP and [11C]β-CFT-FP, selective radioligands for visualisation of the dopamine transporter using positron emission tomography (PET). Journal of Labelled Compounds and Radiopharmaceuticals, 2000, 43, 1235-1244.	1.0	19
151	High specific radioactivity (1R,2S)-4-[18F]fluorometaraminol: a PET radiotracer for mapping sympathetic nerves of the heart. Nuclear Medicine and Biology, 2000, 27, 233-238.	0.6	17
152	Carbon-11 pb-12: an attempt to visualize the dopamine d4 receptor in the primate brain with positron emission tomography. Nuclear Medicine and Biology, 2000, 27, 707-714.	0.6	24
153	Absolute quantitation of iodine-123 epidepride kinetics using single-photon emission tomography: comparison with carbon-11 epidepride and positron emission tomography. European Journal of Nuclear Medicine and Molecular Imaging, 1999, 26, 1580-1588.	6.4	20
154	Precursor synthesis and radiolabelling of the dopamine D2 receptor ligand [11C]raclopride from [11C]methyl triflate. Journal of Labelled Compounds and Radiopharmaceuticals, 1999, 42, 1183-1193.	1.0	105
155	Carbon-11 epidepride: a suitable radioligand for PET investigation of striatal and extrastriatal dopamine D2 receptors. Nuclear Medicine and Biology, 1999, 26, 509-518.	0.6	20
156	Preparation of 4- and 6-[76Br] bromometaraminol, two potential radiotracers for the study of the myocardial norepinephrine neuronal reuptake system with PET. Journal of Labelled Compounds and Radiopharmaceuticals, 1997, 39, 803-816.	1.0	8
157	Some new methods for the synthesis of cardiac neurotransmission PET radiotracers. Nuclear Medicine and Biology, 1995, 22, 1037-1043.	0.6	4